c-Jun NH_2-Terminal Kinase Activating Kinase 1/Mitogen-Activated Protein Kinase Kinase 4–Mediated Inhibition of SKOV3ip.1 Ovarian Cancer Metastasis Involves Growth Arrest and p21 Up-regulation

Tamara Lotan,[1] Jonathan Hickson,[2] Jeffrey Souris,[3,5] Dezheng Huo,[4] Jennifer Taylor,[6] Terry Li,[7] Kristen Otto,[8] Seiko Diane Yamada,[2,5,9] Kay Macleod,[5,6,10] and Carrie W. Rinker-Schaeffer[2,5,6,8,9]

Departments of [1]Pathology, [2]Obstetrics and Gynecology, [3]Radiology, and [4]Health Studies; [5]The University of Chicago Interdepartmental Metastasis Research Group (UCIMRG); [6]Committee on Cancer Biology; [7]Immunology Applications Core Facility; [8]Section of Urology, Department of Surgery; [9]University of Chicago Cancer Research Center; and [10]Ben May Department for Cancer Research, The University of Chicago, Chicago, Illin3ois

Abstract

In many patients without clinical metastases, cancer cells have already escaped from the primary tumor and entered a distant organ. A long-standing question in metastasis research is why some disseminated cancer cells fail to complete steps of metastatic colonization for extended periods of time. Our laboratory identified c-Jun NH_2-terminal kinase activating kinase 1/mitogen-activated protein kinase kinase 4 (JNKK1/MKK4) as a metastasis suppressor protein in a mouse xenograft model of experimental i.p. ovarian cancer metastasis. In this model, expression of JNKK1/MKK4 via activation of p38 delays formation of ≥1-mm implants and prolongs animal survival. Here, we elucidate the time course of this delay as well as the biological mechanisms underpinning it. Using the Gompertz function to model the net accumulation of experimental omental metastases, we show that MKK4-expressing implants arise, on average, 30 days later than controls. Quantitative real-time PCR shows that MKK4 expression does not have a substantial effect on the number of cancer cells initially adhering to the omentum, and terminal deoxyribonucleotidyl transferase–mediated dUTP nick end labeling analysis shows that there is no increase in apoptosis in these cells. Instead, immunohistochemical quantitation of cell cycle proteins reveals that MKK4-expressing cells fail to proliferate once they reach the omentum and up-regulate p21, a cell cycle inhibitor. Consistent with the time course data, *in vitro* kinase assays and *in vivo* passaging of cell lines derived from macroscopic metastases show that the eventual outgrowth of MKK4-expressing cells is not due to a discrete selection event. Rather, the population of MKK4-expressing cells eventually uniformly adapts to the consequences of up-regulated MKK4 signaling. [Cancer Res 2008;68(7):2166–75]

Introduction

This year, 560,000 Americans will die from cancer, most of them from metastatic disease (1). In the majority of patients without detectable metastases, viable tumor cells have already escaped from the primary tumor and entered one or more distant organ sites (2, 3). The high recurrence rate after definitive local therapies, such as cytoreduction for ovarian cancer, shows the urgent need to identify patients at risk for disease recurrence as well as the need for antimetastatic therapies to treat the disease. Clinical and experimental studies have identified the final step in this process, metastatic colonization of secondary sites, as a tractable therapeutic target (4). Mechanisms regulating this clinically important process are being elucidated by studies of metastasis suppressor proteins that can specifically inhibit metastatic colonization (5).

Our laboratory identified c-Jun NH_2-terminal kinase activating kinase 1/mitogen-activated protein kinase (MAPK) kinase 4 (JNKK1/MKK4; hereafter referred to as MKK4) as a metastasis suppressor protein for ovarian cancer using a well-characterized SKOV3ip.1 xenograft model of experimental i.p. metastasis (6). As a key member of the stress-activated protein kinase (SAPK) signaling cascade, MKK4 can itself phosphorylate both the JNK and p38 MAPKs, resulting in the activation of transcription factors including activator protein 1 and activating transcription factor 1 (7, 8). Using SKOV3ip.1 cells (9), a metastatic human ovarian cancer cell line that lacks significant endogenous MKK4, we showed that ectopic expression of hemagglutin (HA)-tagged MKK4 reduces overt experimental metastasis formation by 90% in a kinase-dependent manner and that MKK4 signals through p38, and not JNK, to suppress *in vivo* metastatic colonization (6, 10). As is the case with other metastasis suppressors, SKOV3ip.1 cells expressing HA-MKK4 have no detectable alterations in the rate of growth or apoptosis under a variety of *in vitro* growth conditions (6). Thus, the suppressive effect of MKK4 on metastatic growth is dependent on *in vivo* activation of the protein. Interestingly, animals injected with MKK4-expressing cells show a 70% improvement in survival as compared with controls, but these animals will eventually succumb to disease burden (6, 10).

These findings raise several important questions: What are the biological mechanisms responsible for MKK4-mediated suppression of metastatic colonization? Can MKK4-expressing cells become resistant to the effects of MKK4? Building on our previous work, which supports a mechanism by which MKK4 signals through p38 to suppress metastatic colonization and that its suppressor activity is kinase dependent, we set out to determine how MKK4 acts at the cellular level in the clinically relevant microenvironment of the omentum to inhibit outgrowth of disseminated cells. Experiments were designed to examine how MKK4-expressing cells ultimately bypass this suppression. Using complementary approaches, we show that MKK4 does not significantly decrease the number of cancer cells adhering to the omentum, nor does it increase the number of apoptotic cells. Instead, MKK4-expressing cells attached to the omentum fail to proliferate and show a concomitant up-regulation of the cell cycle

Note: T. Lotan and J. Hickson are co-first authors.
Requests for reprints: Carrie Rinker-Schaeffer, Section of Urology, Department of Surgery, The University of Chicago, 5841 South Maryland Avenue, MC6038, Chicago, IL 60637. Phone: 773-702-5882; Fax: 773-702-1001; E-mail: crinkers@uchicago.edu.

doi:10.1158/0008-5472.CAN-07-1568

inhibitory protein p21. We also show that, contrary to conventional wisdom, the eventual outgrowth of MKK4-expressing cells is not due to a discrete genetic selection event. Rather, our data support a model in which the population of MKK4-expressing cells adapts to the consequences of MKK4 activation and down-regulates p21 expression, eventually forming macroscopic experimental metastases. Discerning the mechanisms that regulate MKK4-mediated suppression of colonization has significant clinical implications for the design of drugs and therapies aimed at controlling disseminated tumor growth. Conversely, understanding how some MKK4-expressing cancer cells bypass suppression and form overt lesions is also critical if we wish to lengthen the interval of suppression. This work represents important progress toward both of these translational goals.

Materials and Methods

Cell lines and culture conditions. Previously characterized SKOV3ip.1-pLNCX2 (vector) and SKOV3ip.1-HA-MKK4 clonal cell lines were maintained in standard conditions (10). To establish metastasis-derived cell lines, individual overt (i.e., ≥1 mm) lesions were excised and placed in 200 μL of dissociation medium [DMEM containing 5% FCS, 1% penicillin (100 units/mL)/streptomycin (100 μg/mL) mixture, 0.25 μg/mL amphotericin (Mediatech), and 12,500 units/mL collagenase (Worthington Biochemical)]. Samples were incubated for ~16 h at 37°C with shaking (200 rpm) to form a homogeneous suspension of dissociated cells. Cells were collected by centrifugation and the pellet washed once with PBS. Cells were resuspended and plated in growth medium in a 10-cm tissue culture dish.

Immunoblotting, immunoprecipitation, and *in vitro* kinase assays. For immunoblotting, 30 μg of total protein were prepared, resolved, transferred, and immunoblotted as previously reported (10). The primary antibodies and dilutions used were as follows: HA.11 (Covance; 1:1,000), p38 (Cell Signaling Technologies; 1:1,000), and phospho-p38 (Cell Signaling Technologies; 1:1,000). Probed membranes were stripped with Restore Western Blot Stripping Buffer (Pierce), washed, and blocked overnight before reprobing. Actin was used as a loading control (Calbiochem; 1:10,000).

To assess MKK4 kinase activity, SKOV3ip.1 cells were cultured in complete growth medium containing 0.1% FCS for 24 h and stimulated with 1 μg/mL anisomycin (Sigma) or ethanol control for 20 min before cell lysis, followed by immunoprecipitation, *in vitro* kinase assays, and resolution by SDS-PAGE (10). As a loading control, membranes were immunoblotted for p38 substrate using the following dilutions: primary (1:20,000), secondary (1:40,000).

Experimental metastasis assays in immunodeficient mice. Female athymic nude mice or beige nude XID (NIH III) mice (Harlan Sprague-Dawley; 4–6 wk old) were used for *in vivo* studies. Cells were not grown beyond 80% confluence before preparation for mouse injection. Cells (1×10^6; 500 μL of a 2×10^6 cells/mL solution) were injected i.p. (6). For determination of *in vivo* growth kinetics, a total of 165 mice were injected with one of three SKOV3ip.1-vector clones (clones 1–3) or four SKOV3ip.1-HA-MKK4 clones (clones 1–4; ref. 10). Every 10 d postinjection (dpi), three to five mice per clone were euthanized and the number of ≥1-mm-diameter metastases assessed during necropsy. SEs at each time point represent the data from 12 to 15 mice. For all other studies, animals were injected with one SKOV3ip.1-vector (clone 3) or HA-MKK4 cell line (clone 2) and sacrificed at the experimental end points (3, 14, 30, or 60 dpi).

Quantitative real-time PCR. Primers and a probe specific to an intronic portion of the human β-globin gene were used to detect human cells in mouse omentum (Integrated DNA Technologies). The sequences were as follows: human β-globin F, 5′-GAGGGTTTGAAGTCCAACTCCTAA-3′; human β-globin R, 5′-CAGGGTGAGGTCTAAGTGATGACA-3′; dual labeled reporter probe, 5′-FAM-ACCTGTCCTTGGCTCTTCTGGCACTG-BHQ-1-3′. To normalize against mouse DNA, mouse-specific primers specific to an intronic portion of β-globin were also designed: mouse β-globin F, 5′-GGCTGCCTGCCTTTAATTCA-3′; mouse β-globin R, 5′-GGTTAGCTTGGATAACCTGCTTTTT-3′; dual labeled reporter probe, 5′-FAM-AGGGATTGTCCTGTCCTTCCACGCTT-BHQ-1-3′. All DNAs were prepared from cells and tissues with the PUREGENE DNA Purification Kit according to the manufacturer's protocol (Gentra Systems). DNA from each omentum (for the standard curve and all experimental samples) was purified into 200-μL Tris-EDTA and subsequently diluted 1:10 before adding 1 μL of DNA to the quantitative reverse transcription-PCR (RT-PCR) reaction. Quantitative RT-PCR reactions were prepared using the Brilliant Probe-Based QRT-PCR Reagents (Stratagene) in a total volume of 25 μL: 2.5 μL 10× core PCR buffer, 4 mmol/L $MgCl_2$, 800 μmol/L deoxynucleotide triphosphates, 500 nmol/L forward primer, 500 nmol/L reverse primer, 200 nmol/L probe, 30 nmol/L ROX reference dye, 1.25 units Surestart Taq polymerase, and ~150 ng DNA template. Reactions were run and data analyzed on the MX3000 QRTPCR system (Stratagene) with a 10-min incubation at 95°C, followed by a two-step reaction: 95°C × 15 s and 64°C × 60 s for 40 cycles. All reactions were done in triplicate, with appropriate negative controls (100% mouse DNA for human primers, 100% human DNA for mouse primers, and water).

Histologic analysis and immunohistochemical staining of experimental metastases. For analysis of microscopic lesions, the omentum was excised from euthanized mice, fixed overnight in 10% neutral buffered formalin, processed, and embedded in paraffin. Tissue sections (5 μm) were prepared and stained with H&E for histologic analysis. Terminal deoxyribonucleotidyl transferase–mediated dUTP nick end labeling (TUNEL) assay was done with the Apoptag Plus *In Situ* Detection Kit as directed by the manufacturer (Chemicon). For immunohistochemical staining, tissue sections were rehydrated in three 5-min xylene washes, two 5-min 100% ethanol washes, and two 5-min 95% ethanol washes. Antigen retrieval was done in the microwave in sodium citrate buffer (pH 6) for all antibodies except for pan-cytokeratin staining, for which enzymatic digestion was done with 1 mg/mL proteinase K in PBS at 37° for 5 min. Endogenous peroxidase activity was blocked with 3% hydrogen peroxide for 15 min. Tissue sections were blocked in 5% goat serum for 1 h at room temperature. For pan-cytokeratin immunostaining, tissue sections were incubated for 1 h at room temperature with a rabbit polyclonal antiserum (1:1,000; DAKO). For bromodeoxyuridine (BrdUrd) and p16 immunostaining, tissue sections were incubated for 1 h at room temperature with a sheep polyclonal antiserum (1:2,000; Research Diagnostics, Inc.) or a mouse monoclonal antiserum (1:200; BD Biosciences), respectively. For phospho-histone H3, p21, and MKK4 immunostaining, sections were incubated at 4° overnight with a rabbit polyclonal antiserum (1:300; Upstate), a mouse monoclonal antiserum (clone SX118; 1:50; BD Biosciences), or a mouse monoclonal anti-MKK4 antibody (1:15; Novocastra Laboratories), respectively. For p27kip1 immunostaining, sections were incubated for 30 min at room temperature with a mouse monoclonal antiserum (clone SX53G8, 1:25; DAKO). Immunolabeling reactions were developed with the EnVision Plus detection system (DAKO) followed by counterstaining with hematoxylin. Mouse colonic mucosa served as a positive internal control for BrdUrd and phospho-histone H3, and tonsil and pancreatic islet cells were used as positive internal controls for p21 and p27kip1 staining, respectively. Tissue from a human nevus was used as a positive control for p16 immunostaining. Negative controls were isotype control rabbit/mouse IgG.

Immunohistochemical data analysis. For BrdUrd and phospho-histone H3 immunostaining of the 14 dpi omenta and p21 and p27 immunostaining of the 30 dpi omenta, an automated, computer-assisted image analysis system was used to score percentage of nuclei with positive staining (Chromavision). Immunostained histologic sections of each omentum were digitally scanned into the system at ×10 magnification, and each microscopic metastasis (14 dpi) was manually identified and scored for size (μm^2) and percentage of positively stained cells. For the 30 dpi omenta, multiple 10× fields were randomly chosen and scored for percentage of positively stained cells. For p21 and p27 immunostaining of the 14 dpi omenta, higher background staining necessitated manual scoring of tumor cells in each microscopic metastasis.

Mathematical modeling of *in vivo* growth kinetics in the SKOV3ip.1 model. A least squares nonlinear regression, based on the Marquardt-Levenberg algorithm for the iterative estimation of coefficients, was used to fit the number of overt implants observed in mice injected with either

SKOV3ip.1-vector (60 mice) or SKOV3ip.1-HA-MKK4 (105 mice) cells to a three-parameter Gompertz curve of the form

$$N_i(t) = N_{\max,i} e^{-e^{-(t-t_{o,i})/b_i}}$$

.

Here, the index i is used to distinguish vector from HA-MKK4; N_i *(t)* is the total number of overt (≥1 mm diameter) metastases present in the animal at time t; $t_{o,i}$ is the offset/delay time parameter; b_i is the growth rate normalization parameter, indicating the steepness of the Gompertz curve; and $N_{\max,i}$ is the maximum total number of overt metastases an animal can support irrespective of time [the asymptote $N_i(t)$ approaches as $t \to \infty$]. Huber/White robust standard errors were used to account for the intra-clone correlation. This sigmoidal model has previously been applied to describe the growth kinetics of cancer cells *in vitro* and primary tumors *in vivo* (11, 12). It is more biologically feasible than a simple exponential model because the doubling time for metastasis number changes over time (initially increases and then decreases) and it does not assume that the number of metastases increases infinitely.

Statistical analyses. First, the numbers of SKOV3ip.1-vector and SKOV3ip.1-HA-MKK4 cells present on the omentum 3 dpi were compared using a nonparametric Wilcoxon rank-sum test. Second, to stabilize the variance and normalize the data, a log transformation was applied to the size of metastases and an arcsine-root transformation was applied to the proportion of positive immunohistochemical staining of implants (TUNEL, BrdUrd, phospho-histone H3, p21, and p27) before further analysis, although results are still presented in original scale. Size of implants and proportion of positive staining cells were compared between the vector and HA-MKK4 groups using mixed effect linear models, treating each animal as a random effect because observations within each animal may be correlated. If the random effect was found be nonsignificant based on likelihood ratio test, the mixed effect model was reduced to a two-sample t test. Third, two-way analysis of variance was used to compare number of implants 30 dpi between vector and HA-MKK4 in both athymic nude mice and NIH III mice following a square root transformation on the number of implants. Finally, following square root transformation, the number of implants 30 dpi from the metastasis-derived HA-MKK4 cells lines (clones), the parental HA-MKK4 cell line, and a vector control were compared using a mixed effect linear model in which each clone was treated as random effect (because mice within each experiment were correlated). The Tukey multiple comparison procedure was used to adjust for multiple pairwise testing.

Results

Modeling the growth delay of MKK4-expressing cells. Expression of HA-MKK4 in SKOV3ip.1 cells significantly reduces the number of overt implants following i.p. injection and extends animal survival (6, 10). Eventually, however, even mice injected with HA-MKK4–expressing cells develop macroscopic metastases and succumb to their disease burden. We posited that mathematical analysis of these population-dependent events could assist in the formulation of hypotheses about how MKK4 suppresses colonization and how cells eventually overcome its suppressive effects. To this end, an *in vivo* time course assay was conducted to determine the rate of accumulation of overt experimental metastases in the SKOV3ip.1 model, as well as the extent and duration of suppression by MKK4 (Fig. 1). Animals injected with SKOV3ip.1-vector only cells (Fig. 1, –○–) had ~20 to 30 metastatic implants at 20 dpi, and by ~40 dpi animals succumb to the disease with 80 to 100 overt peritoneal metastases. As previously observed, animals injected with SKOV3ip.1-HA-MKK4 cells (Fig. 1, - -◆- -) showed only ~1 to 2 implants at 20 dpi and did not have 80 to 100 metastases until ~70 dpi.

Using all 165 data points, the kinetics of overt implant formation by both vector-only and HA-MKK4–expressing cells was mathematically modeled with the 3-parameter Gompertz function. In the saturated model with separate parameters ($N_{\max,i}$, $t_{o,i}$, b_i) for MKK4 and vector groups, $N_{\max}$ was not statistically significantly different between MKK4 and vector groups, suggesting that the ultimate burden of experimental metastases each animal faces does not depend on MKK4 expression. The reduced Gompertz model with same $N_{\max}$ (= 245.72) and the other two parameters varied by vector ($t_{o,i}$ = 40.83, b_i = 22.33) and MKK4 ($t_{o,i}$ = 72.21, b_i = 28.39) fit the data well (Fig. 1; coefficient of determination R^2 = 0.883). There was only a marginally significant difference in the overall shapes of the growth curves between vector-only and HA-MKK4–expressing cells (P = 0.087, for b_i between the two groups). Rather than necessitating a separate equation, the HA-MKK4 growth curve was simply shifted in time, with formation of experimental metastases delayed by an average of 30 days (P = 0.003, for $t_{o,i}$ between the two groups). This suggested that suppression and outgrowth of HA-MKK4 cells are due to the uniform behavior of the population and not to the selection of a subset of cells, as would occur with increased apoptosis or differential adhesion of cells to target tissues. The *in vivo* growth curve also indicated that the rate-limiting step in the development of overt metastases in MKK4-mediated suppression occurs in the first 20 dpi, after which animals injected with MKK4-expressing cells begin to accumulate overt implants at a rate similar to control cells. Based on these findings, we formulated three hypotheses: First, similar numbers of SKOV3ip.1-vector and SKOV3ip.1-HA-MKK4 cells attach to the omentum and survive. Second, SKOV3ip.1-HA-MKK4 cells will have a decreased proliferation rate as compared with the vector controls. Finally, outgrowth of HA-MKK4–expressing cells is due to an adaptative response of the population of cells and not selection of cells that have deleted or inactivated the HA-MKK4 transgene.

MKK4 expression does not have a substantial effect on the number of SKOV3ip.1 cells adhering to the omentum. *In vivo* growth of SKOV3ip.1 cells recapitulates the metastatic pattern of

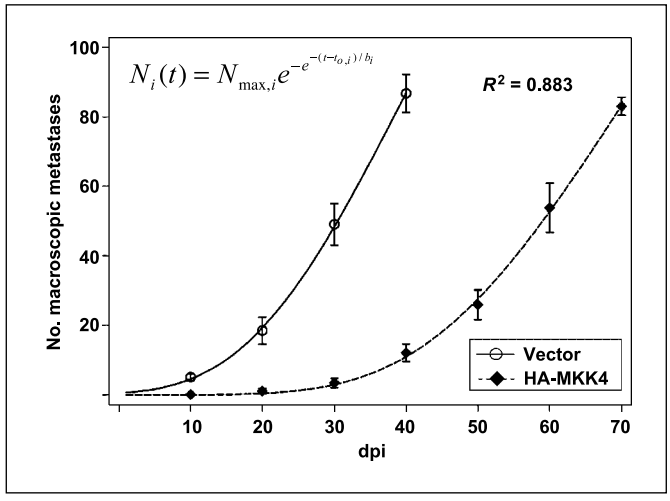

Figure 1. HA-MKK4–expressing cells are delayed in forming macroscopic metastases. The number of ≥1-mm metastases present as a function of time was determined by injecting SKOV3ip.1-vector (–○–) clones or SKOV3ip.1-HA-MKK4 (- -◆- -) clones i.p. into athymic nude mice and assessing the number of metastases every 10 d. *Points,* mean from 12 to 15 mice per time point; *bars,* SE. Nonlinear regression revealed that a three-parameter Gompertz model (*inset*) fit the 165 data points well (R^2 = 0.883), indicating that the shape of growth curve was similar between the two groups. HA-MKK4 cells showed an ~30-day delay in macroscopic metastasis formation compared with vector-only controls.

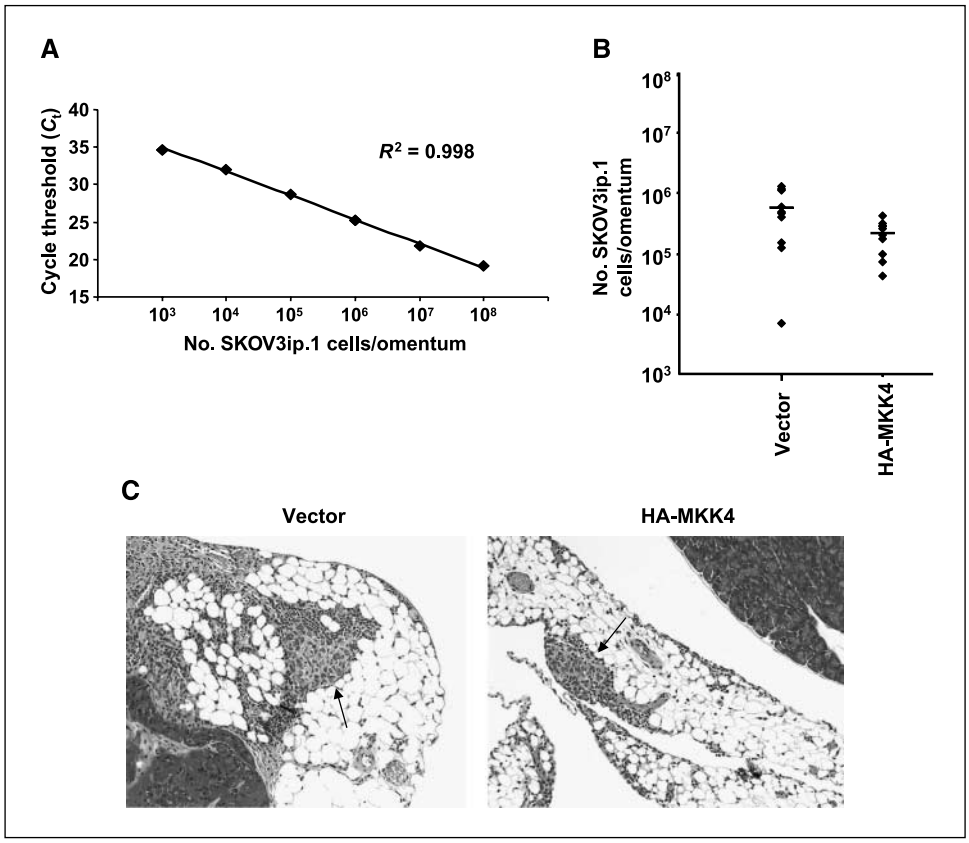

Figure 2. HA-MKK4–expressing and vector-only SKOV3ip.1 cells initially adhere to the omentum in similar numbers. *A,* a quantitative RT-PCR assay was designed to specifically amplify an intronic sequence in the human, but not mouse, β-globin gene. A standard curve was developed by mixing SKOV3ip.1 cell lysates with mouse omentum lysates, showing a range of detection between 1×10^3 and 1×10^8 SKOV3ip.1 cells. *B,* the number of SKOV3ip.1 cells present on the omenta from mice at 3 dpi was quantitated by quantitative RT-PCR assay. Data show that there are approximately twice as many vector-only cells adhering to the omenta as compared with HA-MKK4–expressing cells ($P = 0.06$). *C,* histologic sections of tumor implants show similarly sized tumor nodules in the two groups at 3 dpi (*arrows*; magnification, ×200).

human disease (6). In the experimental metastasis assay, MKK4 expression significantly delays the presentation of overt metastases; however, once HA-MKK4–expressing cells begin to form overt lesions, the temporal and spatial distribution of tumor burden is comparable to control cells (data not shown). To determine whether the delay in formation of SKOV3ip.1-HA-MKK4 experimental metastases is due to decreased adherence of injected cells, a quantitative real-time PCR assay was developed to quantitate the number of cells present on the omentum at 3 dpi. A standard curve was generated using genomic DNA from samples containing known numbers of SKOV3ip.1 (human) cells combined with mouse omentum homogenates, showing a range of detection spanning 10^3 to 10^8 SKOV3ip.1 cells in a background of mouse genomic DNA (Fig. 2*A*). At 3 dpi, there was not a significant difference between the numbers of vector-only and HA-MKK4–expressing cells present on the mouse omentum (vector mean, 5.8×10^5 cells; HA-MKK4 mean, 2.2×10^5 cells; $P = 0.06$; Fig. 2*B*). Further, the modest increase in the number of adherent vector-only cells at this time point was insufficient to account for the 10- to 20-fold decrease in macroscopic metastases formed by HA-MKK4–expressing cells at 20 dpi. Histologic sections of omental tumor implants at 3 dpi revealed discrete tumor nodules without any apparent size differences between the two groups, consistent with the RT-PCR data (Fig. 2*C*). Thus, MKK4-mediated suppression of metastatic colonization is not due to decreased adhesion of cells to the omentum.

Apoptosis is not increased in HA-MKK4–expressing microscopic metastases. To address the possibility that MKK4 induces apoptosis in SKOV3ip.1 cells once they have adhered to i.p. structures, histologic sections of early implants (14 dpi) were prepared and TUNEL reaction was done. At 14 dpi, vector-only implants are ~10 times larger than those composed of HA-MKK4–expressing cells on histologic cross section ($P < 0.0004$, Fig. 3*A*), confirming that the MKK4-mediated growth delay is already occurring. Quantification of TUNEL-positive cells in >25 vector-only or HA-MKK4–expressing microscopic foci (from seven to eight animals each) revealed only rare apoptotic cells (<1%) in both groups ($P = 0.43$; Fig. 3*B*). Histologic examination of HA-MKK4–expressing microscopic foci at this time point revealed an inflammatory infiltrate composed of lymphocytes, histiocytes, and plasma cells surrounding the tumor cells in the athymic nude mice, with tumor foci highlighted by pan-cytokeratin immunostaining (Fig. 3*A*). Although nude mice have significantly decreased numbers of functional T cells, they retain a complement of B cells as well as increased levels of natural killer (NK) cells and macrophages (13). To address the possibility that HA-MKK4–expressing cells may preferentially invoke host immune response, leading to impaired proliferation, experimental metastasis assays were also conducted in beige nude XID (NIH III) mice, which lack functional T cells, B cells, and NK cells (14). By 30 dpi, beige nude XID (NIH III) mice injected with HA-MKK4–expressing cells show suppression comparable to that in athymic controls ($P < 0.0001$, HA-MKK4 compared with vector-only control; Fig. 3*D*) despite the lack of significant inflammatory infiltrate surrounding the keratin-positive tumor cells (Fig. 3*C, arrows*). Taken together, these studies allowed us to exclude induction of apoptosis or host immune response as being involved in MKK4-mediated suppression.

HA-MKK4–expressing microscopic implants show decreased proliferation. To address the possibility that MKK4-expressing cells are deficient in proliferation, SKOV3ip.1 vector-only and

HA-MKK4 cells were injected into athymic nude mice, and at 14 dpi, animals were injected with BrdUrd, subsequently sacrificed, and microscopic lesions were assessed for BrdUrd incorporation (a marker of S-phase cells) and phospho-histone H3 expression (a marker of M-phase cells). Analysis of >160 microscopic lesions expressing either vector-only or HA-MKK4 revealed that BrdUrd incorporation was significantly decreased in HA-MKK4–expressing cells (Fig. 4*A* and *B*; average of 6% versus 19% positive cells, $P < 0.0001$). Similarly, phospho-histone H3 staining showed decreased numbers of mitotic HA-MKK4–expressing cells (Fig. 4*C* and *D*; average of 0.7% versus 2.5% positive cells, $P = 0.004$). Consistent with our hypotheses, MKK4-expressing cells show decreased proliferation.

HA-MKK4–expressing microscopic metastases have increased levels of p21. The decrease in both BrdUrd incorporation and phospho-histone H3–positive cells in HA-MKK4–expressing microscopic lesions suggested that fewer cells were traversing S phase and subsequently M phase compared with controls. This finding, coupled with the fact that these cells eventually proliferate to form macroscopic implants, is consistent with a reversible cell cycle arrest. This prompted us to study the expression of cell cycle inhibitory proteins potentially acting in the HA-MKK4–expressing microscopic lesions. SKOV3 cells are known to be null for a variety of cell cycle inhibitors including p53 and p16 (15–17); thus, protein expression of p21(Waf1/Cip1) and p27(Kip1) was quantified in HA-MKK4–expressing microscopic metastases at 14 dpi. p16 immunostaining provided a negative control for this series of experiments (Fig. 5*A*). This approach revealed that p21 expression was increased nearly 10-fold in HA-MKK4–expressing microscopic lesions compared with vector-only controls (average of 9% versus 1%, $P < 0.0001$; Fig. 5*B*). Nuclear p27 was only modestly increased in HA-MKK4–expressing cells and was of marginal statistical significance (average of 5% versus 1%, $P = 0.03$; Fig. 5*C*). Given that only a proportion of the total population of SKOV3ip.1 cells are in cell cycle at any given time point (with 19% entering S phase in a 4-hour window), the observed increase in p21 immunostaining (9% of the population) is biologically relevant and, combined with decreased BrdUrd incorporation and phospho-histone H3 staining, is consistent with our hypothesis that MKK4-mediated suppression of colonization is due to impaired cellular proliferation.

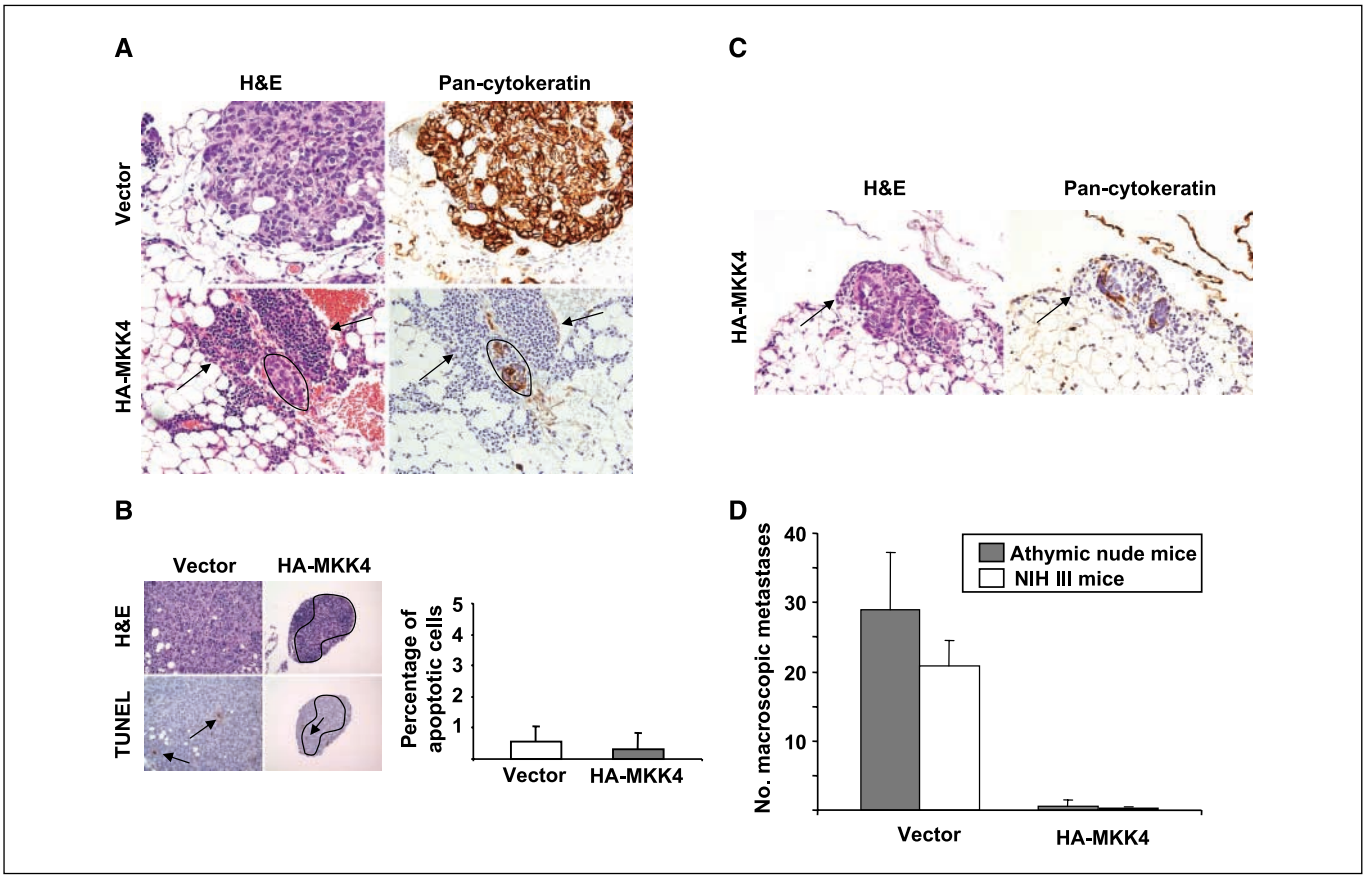

Figure 3. The *in vivo* growth delay of HA-MKK4–expressing cells cannot be attributed to increased apoptosis or surrounding host immune infiltrate. *A,* a quantitative histologic assessment of tissues scanned at ×100 magnification showed that by 14 dpi, vector-only metastases are ~10-fold larger than HA-MKK4–expressing metastases ($P < 0.0004$). HA-MKK4–expressing microscopic metastases (*bottom*, delineated by black circles; ×400 magnification) are surrounded by an inflammatory infiltrate composed of lymphocytes, histiocytes, and plasma cells in the athymic nude mice (*arrows*), and tumor cells are highlighted by pan-cytokeratin staining (*right*). *B,* TUNEL reaction for apoptotic cells shows only rare positive cells (*left, arrows*) in both groups (magnification, ×200). Quantification of TUNEL-positive cells (*right*) in >25 vector-only or HA-MKK4–expressing metastases arising in seven to eight animals each revealed <1% apoptotic cells in both groups ($P = 0.43$). *C,* at 14 dpi, beige nude XID (NIH III) mice injected with HA-MKK4–expressing cells showed microscopic metastases comparable in size and histology to those in athymic nude mice but with only a scant inflammatory infiltrate (*left, arrow*; ×400 magnification). Tumor cells are highlighted by pan-cytokeratin immunostaining (*right*). *D,* by 30 dpi, HA-MKK4–expressing cells were similarly suppressed for macroscopic metastasis formation in NIH III mice compared with athymic controls ($P < 0.0001$, for HA-MKK4 in both groups of mice compared with vector-only controls; $n = 5$ for each bar in graph).

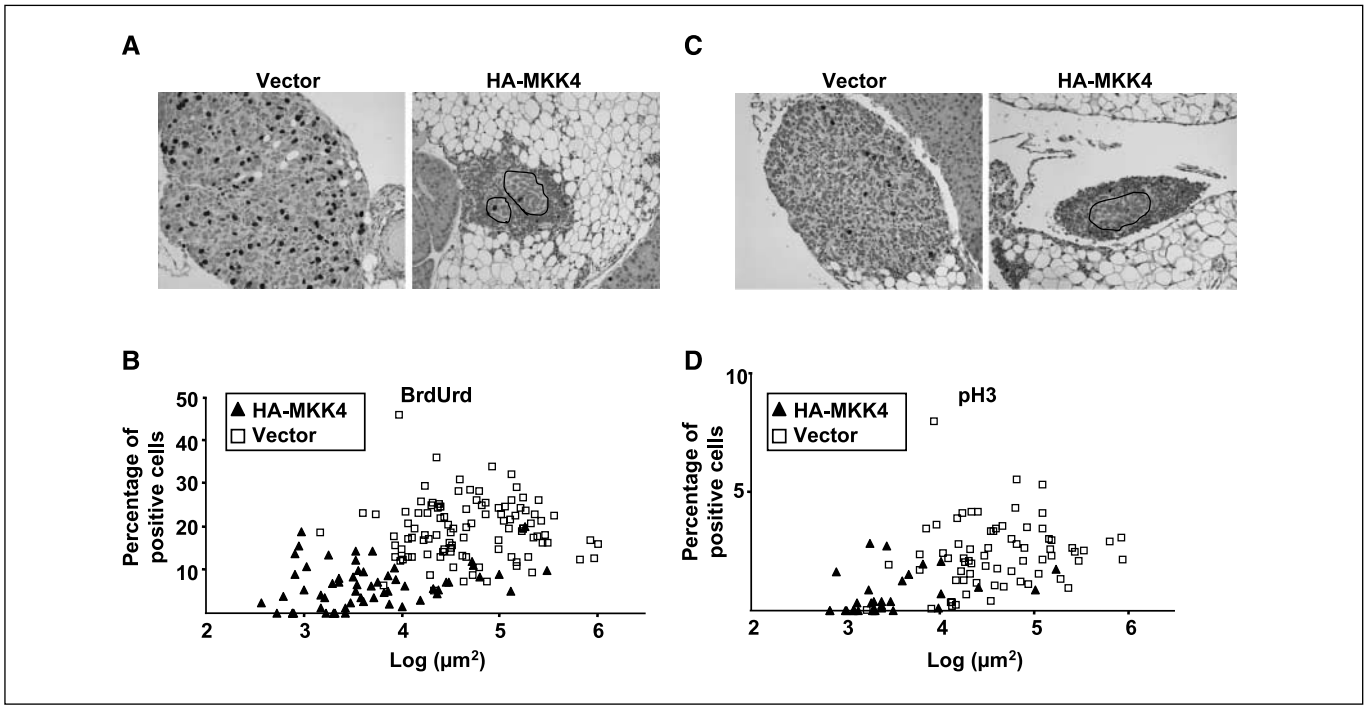

Figure 4. HA-MKK4–expressing microscopic metastases show decreased proliferation as assessed by BrdUrd incorporation and phospho-histone H3 staining at 14 dpi. *A,* BrdUrd was injected i.p. 4 h before the experimental end point. Immunolabeling for BrdUrd in vector-only and HA-MKK4–expressing SKOV3ip.1 microscopic metastases at 14 dpi (×100 magnification). *B,* more than 160 microscopic metastases were scored for size (in square micrometers) and percent BrdUrd-positive cells using a computer-aided image analysis system. Both size and BrdUrd incorporation were significantly decreased in HA-MKK4–expressing metastases compared with vector-only metastases ($P = 0.0003$ and $P < 0.0001$, respectively). *C,* immunolabeling for phospho-histone H3 in vector-only and HA-MKK4–expressing SKOV3ip.1 microscopic metastases at 14 dpi (×100 magnification). *D,* more than 100 microscopic metastases were scored for size (in μm^2) and percent phospho-histone H3 (*pH3*)–positive cells using a computer-aided image analysis system. Both size and phospho-histone H3 immunostaining for mitotic cells were significantly decreased in MKK4-expressing metastases compared with vector-only metastases ($P = 0.0008$ and $P = 0.004$, respectively).

Metastasis-derived SKOV3ip.1-HA-MKK4 cell lines retain expression of functional MKK4 protein and remain suppressed for metastatic colonization when repassaged through naïve mice. Our data that both vector only– and HA-MKK4–expressing populations of experimental metastases undergo uniform expansion suggested that the eventual outgrowth of HA-MKK4–expressing cells is the result of a population-wide adaptation to the consequences of SAPK signaling. This model prompted the hypothesis that the outgrowth of HA-MKK4–expressing cells was not due to selection of cells having deleted or functionally inactivated HA-MKK4. To test this, overt implants arising from HA-MKK4–expressing SKOV3ip.1 cells at ~65 dpi were evaluated by immunostaining (Fig. 6*A*). The data show that these overt experimental metastases do, in fact, continue to express HA-MKK4, indicating that no selection occurred (Fig. 6*A*). To expand on these findings, 25 independent metastasis-derived cell lines were established from mice injected with HA-MKK4–expressing SKOV3ip.1 cells. Continued expression of HA-MKK4 in these metastasis-derived cell lines was confirmed by immunoblotting for the HA-epitope tag (representative data are shown in Fig. 6*B*). By kinase assay, all of the SKOV3ip.1-HA-MKK4 metastasis-derived cell lines retained biochemically functional HA-MKK4 and phosphorylated p38 (representative data shown in Fig. 6*B*).

Although metastasis-derived SKOV3ip.1-HA-MKK4 cell lines retain expression of HA-MKK4, which can be artificially activated *in vitro*, it is possible that these cells have undergone other permanent molecular changes that will inactivate the MKK4 signaling module of the SAPK signaling pathway. If selection is indeed occurring, reinjection of these cell lines in our standard experimental metastasis assay should result in increased experimental metastasis formation compared with the parental HA-MKK4–expressing SKOV3ip.1 clones. To this end, metastasis-derived SKOV3ip.1-HA-MKK4 cell lines were assayed *in vivo*. Compared with vector-only cells, MKK4 metastasis-derived lines were still suppressed in their ability to form overt experimental metastases (mean of 29.6 ± 8.1 versus 4.8 ± 5.5, $P < 0.0001$) when reinjected into naïve mice (Fig. 6*C*). Taken together, these *in vitro* and *in vivo* data strongly suggest that the eventual outgrowth of HA-MKK4–expressing cells is not due to selection for clones of cells that have permanently altered their MKK4 signaling status, but is rather due to adaptation of the population to the biological consequences of SAPK signaling. Consistent with this idea, p21 protein expression is down-regulated in the overt HA-MKK4–expressing implants (30 dpi; Fig. 6*D*) compared with the earlier levels of expression in the microscopic metastases (14 dpi; Fig. 5*A*). In fact, by 30 dpi, there was no difference in p21 expression between HA-MKK4 and vector-only cells ($P = 0.49$; Fig. 6*D*). Collectively, these studies support the hypothesis prompted by the kinetic analysis that outgrowth of HA-MKK4–expressing cells is due to a population-wide adaptation of the cells to microenvironmental stimuli.

Discussion

Understanding the function of metastasis suppressor proteins can potentially help to identify patients at risk for progressive

metastasis development as well as identify antimetastatic therapies. Our laboratory and others identified MKK4 as a metastasis suppressor protein in clinical and experimental ovarian cancers. Immunolabeling of human tissues showed that MKK4 protein expression is significantly down-regulated in ovarian cancer metastatic implants compared with normal ovarian epithelium (6). *In vitro*, MKK4 expression does not affect inherent proliferation or increase cell death of SKOV3ip.1 cells (6). Rather, cumulative findings show that MKK4 exerts its effect in a context-dependent manner *in vivo* (10).

Since our initial report of the metastasis suppressor activity of MKK4, other laboratories have also examined its presence and expression in a variety of malignancies. For example, a recent study using digital karyotyping of clinical ovarian carcinoma specimens identified the MKK4 locus as a deleted "common" target of small interstitial deletions on human chromosome 17, and down-regulation of MKK4 is frequently observed in ovarian serous carcinoma tissues (18). Moreover, differential expression array analysis identified high MKK4 expression as a predictor of improved response to surgical debulking of ovarian cancers (19). Despite the considerable clinical and biochemical evidence for a role for MKK4 in inhibiting the spread of ovarian cancer, a number of important questions remained unanswered at the inception of the current work.

What are the biochemical and biological mechanisms by which activated MKK4 suppresses metastasis formation? An inherent property of signaling molecules is that their activation is dependent on the strength and duration of specific environmental stimuli. Consistent with this fundamental attribute of signaling kinases, JNKK1/MKK4 protein is only activated and functional when an appropriate external signal is received. In the case of suppression of experimental metastasis formation, this signal is provided to SKOV3ip.1-HA-MKK4 cells by interaction with the *in vivo* microenvironment. Building on our previous findings that MKK4 signals through the p38 MAPK to suppress experimental metastasis formation, we set out to determine how MKK4 acts at the cellular level to inhibit this process. A kinetic analysis of metastatic growth allowed us to formulate testable hypotheses about the rate-limiting steps involved in suppression of metastatic colonization. Complementary studies found that MKK4-mediated growth arrest of cancer cells was associated with up-regulation of p21 expression. Surprisingly, despite the fact that p38 has a well-established role in apoptosis (20, 21), we failed to detect any effect of MKK4 expression on the incidence of cell death in disseminated tumor cells on the omentum. Similarly, decreased adhesion of cells to the omentum does not play a significant role in suppression.

How might p21 up-regulation play a role in suppression of SKOV3ip.1 metastatic colonization? The association between MKK4-mediated suppression of colonization and up-regulation of p21 in the present study is intriguing. The p21 cell cycle inhibitor was originally identified as a p53 target gene (22), a protein that interacted with cyclin-dependent kinase (CDK; ref. 23), and a protein that is markedly up-regulated in cellular senescence (24, 25). Like many tumor cell lines, SKOV3ip.1 cells lack functional p53, and thus up-regulation of p21 in this system is necessarily p53 independent (16). Previous work has shown that p21 can be induced by p53-independent mechanisms (26), including induction by the p53-related molecule p73 (27). However, at least one recent study has suggested that SKOV3 cells do not express p73 (28). This finding needs to be addressed in our model system. In the absence of p53 and p73, p21 levels could be affected by posttranslational mechanisms that regulate p21 protein stability. Interestingly, recent

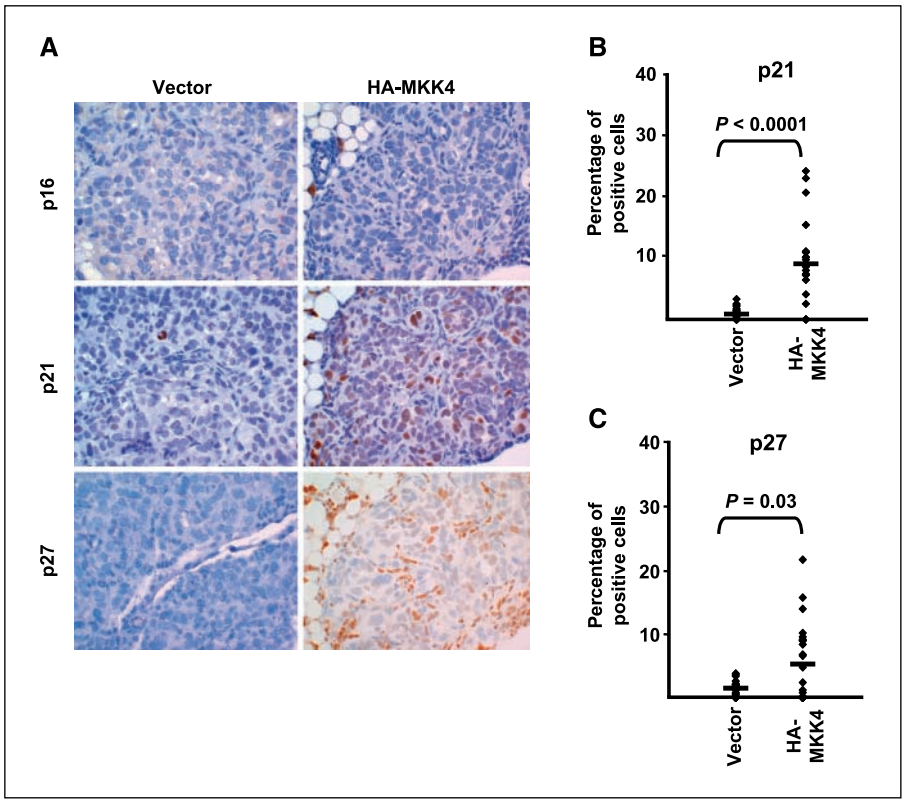

Figure 5. HA-MKK4–expressing microscopic metastases show increased p21 expression at 14 dpi. *A,* immunohistochemical staining for p16, p21, and p27 expression in day 14 metastases (×200 magnification). *B,* p21 nuclear expression was scored in >20 individual microscopic metastases from eight mice injected with either vector-only or HA-MKK4–expressing SKOV3ip.1 cells at 14 dpi. The mean percent of positive cells in SKOV3ip.1 cells vector-only and HA-MKK4 was 1% and 9%, respectively ($P < 0.0001$). *C,* p27 nuclear expression was scored in >20 individual microscopic metastases from three to five mice with either vector-only or HA-MKK4–expressing microscopic metastases at 14 dpi. The mean percent of positive cells in vector-only versus HA-MKK4–expressing cells was 1% and 5%, respectively ($P = 0.03$).

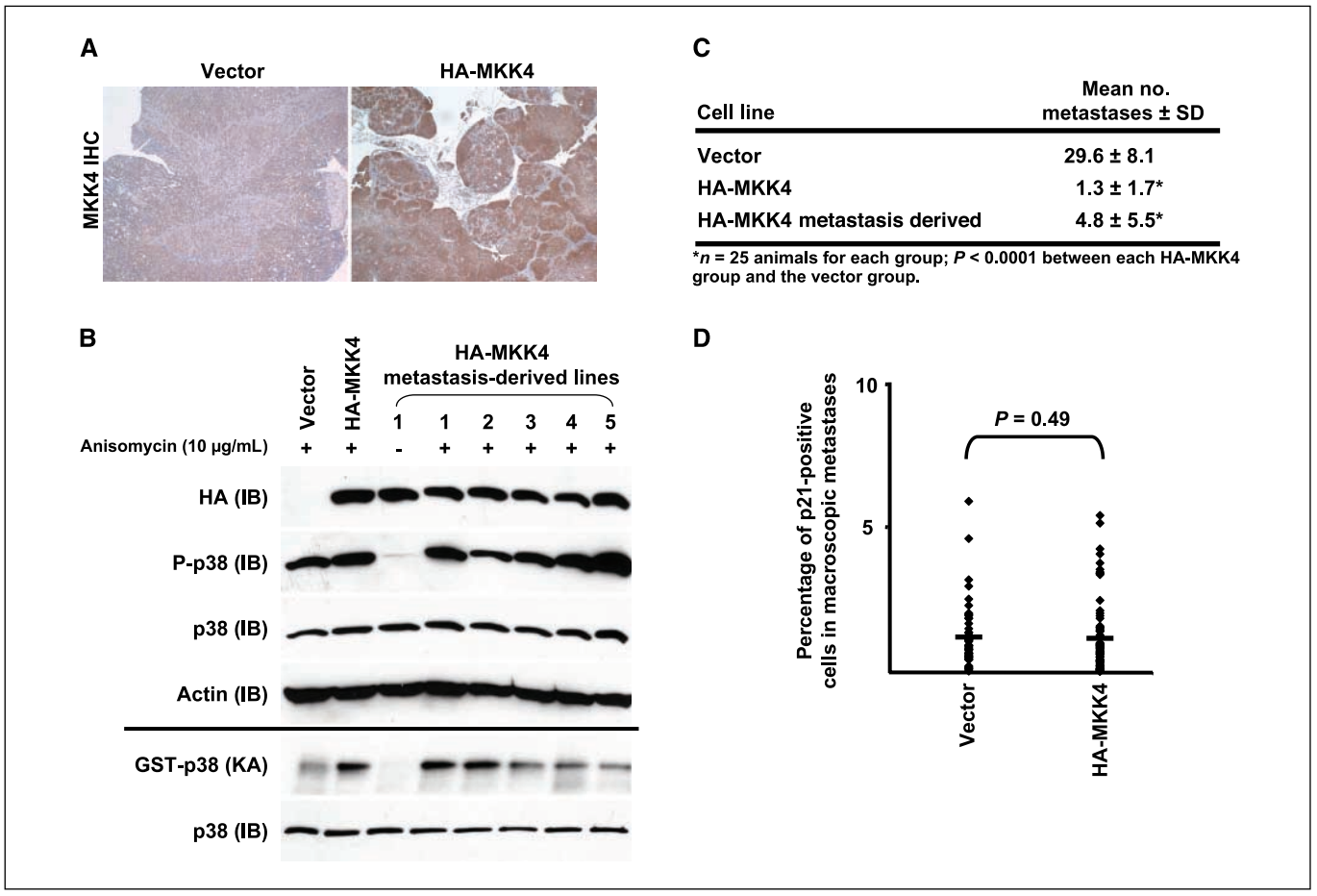

Figure 6. Cell lines derived from macroscopic metastases developing in animals injected with HA-MKK4–expressing SKOV3ip.1 cells retain expression of functional MKK4 *in vitro* and remain suppressed for metastasis when reinjected into naïve mice. *A,* immunohistochemical staining for MKK4 in macroscopic metastases derived from vector-only and HA-MKK4–expressing cells at 30 and 65 dpi, respectively (×40 magnification). SKOV3ip.1 cells have low endogenous MKK4 levels, as seen here in vector-only cells. MKK4 was consistently detected in macroscopic HA-MKK4 metastases. *B,* clonal cell lines were derived from >25 independent SKOV3ip.1-HA-MKK4 macroscopic metastases and screened for the presence of HA-tag, endogenous phospho-p38, p38, and actin after stimulation with anisomycin (representative data are shown). In addition, *in vitro* kinase assays (*KA*) were done to confirm that the HA-MKK4 protein is functional. Kinase assays show that HA-MKK4 is functional *in vitro* and phosphorylates glutathione *S*-transferase (GST)-p38 substrate in a manner similar to parental cell line controls (positive control; *second lane*). As a loading control, the blot was also probed for the GST-p38 substrate (*bottom*). *IB,* immunoblot. *C,* all five metastasis-derived cell lines in *B* were reinjected into five mice each for the standard end-point metastasis assay. These cell lines were equally suppressed for macroscopic metastasis formation at 30 dpi compared with parental lines ($P < 0.0001$, for both groups compared with vector control). *D,* quantitation of p21 immunolabeling in macroscopic metastases (30 dpi) from vector- and HA-MKK4–expressing cells. Sixty to eighty separate 10× fields in macroscopic metastases were scored for p21 immunolabeling on an automated image analysis system from six to seven animals in each group. p21 expression is comparable in both groups by the time macroscopic metastases have developed ($P = 0.49$) and is down-regulated in HA-MKK4–expressing cells by 30 dpi compared with the same cells at 14 dpi (Fig. 5).

in vitro studies have established a biochemical link between SAPK activation and p21 protein levels (29–31). Kim et al. (30) showed that p38-α induced phosphorylation of p21 at Ser^{130} *in vivo* and promoted p21 stabilization, thereby showing a connection between p38 activation and p21 up-regulation.

Taken together, these studies support the notion that p21 may play an important role in MKK4-mediated suppression of metastatic colonization. However, additional studies will be required to elucidate the precise mechanism of this effect. Notably, p21 has a known role in both reversible cell cycle arrest and irreversible cellular senescence. p21 promotes cell cycle arrest *in vivo* through inhibition of CDK activity and activation of pRb in response to numerous signals including DNA damage (32), cytokine signaling (33), and cellular aging (34). The fact that the cell cycle arrest associated with MKK4 expression in our system is apparently reversible, with eventual outgrowth of MKK4-expressing metastases, suggests that the observed growth arrest is not due to cellular senescence. Given that SKOV3ip.1 cells retain functional pRb (17), which is essential for senescence, our work suggests that we may be able to restore the capacity for permanent growth arrest by preventing the eventual down-regulation of p21. In fact, there are currently agents under study *in vitro* and in early clinical trials that specifically target p21 (35, 36).

As the molecular mechanisms of other metastasis suppressor proteins are increasingly well characterized, there is evidence that p21 overexpression and subsequent cellular growth arrest/senescence may mediate suppression in multiple systems. Recently, the metastasis suppressor protein CD82, also known as KAI1, was reported to enable disseminated cancer cells to attach to the vascular endothelial cell surface through interaction with the Duffy antigen receptor for chemokine protein (37–39). This interaction inhibits tumor cell proliferation through induction of senescence with associated up-regulation of p21. Together with the data presented for MKK4, this potentially represents a conserved

biological mechanism underlying the function of multiple metastasis suppressor proteins.

How do MKK4-expressing cells escape suppression and what approaches might be implemented to augment its antimetastatic effects? An important but infrequently discussed consideration in the development of antimetastatic therapies based on metastasis suppressor protein function is how cells may ultimately escape or bypass suppression. A long-standing paradigm of metastasis biology is that the process of both spontaneous and experimental metastasis selects for clones that have undergone permanent molecular changes (such as DNA mutation or deletion) enabling them to complete all steps of the metastatic cascade. Studies were conducted to address the possibility that outgrowth of MKK4-expressing metastases was due to such a canonical selective process. Data presented here show that this is not the case. Careful evaluation of the accumulation of overt experimental metastases over time in our model system showed that MKK4 expression does not significantly affect the overall shape of the metastatic growth curve. Further, MKK4 protein expression is retained in overt metastases and their derived cell lines; the MKK4 protein is functional in standard biochemical assays; and MKK4-expressing metastasis-derived cell lines remain suppressed when reinjected into naïve mice. These results suggest that the population of MKK4-expressing cells homogeneously adapts to the consequences of SAPK signaling and eventually down-regulates p21, enabling outgrowth of metastases.

These novel findings have strong relevance with respect to the dynamic and reciprocal interactions between cancer cells, stromal cells, and other microenvironmental components. In our model system, SKOV3ip.1 cells expressing MKK4 may become resistant to an external stimulus by secretion of a paracrine factor or perhaps by modulating their microenvironment through mechanisms such as stromal reprogramming. We are currently developing complementary *in vivo* and *in vitro* approaches to identify the specific cellular (e.g., host cell-cancer cell interactions), molecular (e.g., matrix components), and physical factors (e.g., cancer cell number and or density), which contribute to activation of MKK4 in SKOV3ip.1 cells during early time points in the process of metastatic colonizaton. Discerning the global and specific processes involved will yield important information about the temporal and spatial activation of MKK4 metastasis suppressor function. MKK4 and other metastasis suppressor proteins with well-characterized biochemical functions may provide new molecular tools for the dissection of the population-dependent interactions of the cancer cells with their microenvironment. Ultimately, it is our goal to use this information to extend the duration of suppression of metastatic colonization. Such findings could have significant implications for the control of clinical ovarian cancers.

Acknowledgments

Received 4/27/2007; revised 12/4/2007; accepted 1/16/2008.

Grant support: The University of Chicago RESCUE Fund (C.W. Rinker-Schaeffer); Department of Defense Ovarian Cancer Research grants DAMD17-03-1-0169 (J. Hickson and S.D. Yamada) and W81XWH-06-1-0041 (C.W. Rinker-Schaeffer), NIH grant RO1 CA 89569 (C.W. Rinker-Schaeffer and J. Hickson), and the Gynecologic Cancer Foundation/Ann Schreiber Ovarian Cancer Research Grant (J. Hickson).

The costs of publication of this article were defrayed in part by the payment of page charges. This article must therefore be hereby marked *advertisement* in accordance with 18 U.S.C. Section 1734 solely to indicate this fact.

We thank Drs. Karl Matlin, Walter Stadler, and Patricia Steeg for their comments; Dr. Theodore Karrison for his statistical insights on this article; and Dr. Arieh Shalhav and the University of Chicago Section of Urology for their strong and unwavering support.

References

1. Cancer facts & figures 2007. Atlanta: American Cancer Society; 2007.
2. Steeg PS. Tumor metastasis: mechanistic insights and clinical challenges. Nat Med 2006;12:895–904.
3. Pantel K, Alix-Panabieres C. The clinical significance of circulating tumor cells. Nat Clin Pract Oncol 2007;4:62–3.
4. Chambers AF, Groom AC, MacDonald IC. Dissemination and growth of cancer cells in metastatic sites. Nat Rev Cancer 2002;2:563–72.
5. Rinker-Schaeffer CW, O'Keefe JP, Welch DR, et al. Metastasis suppressor proteins: discovery, molecular mechanisms, and clinical application. Clin Cancer Res 2006;12:3882–9.
6. Yamada SD, Hickson JA, Hrobowski Y, et al. Mitogen-activated protein kinase kinase 4 (MKK4) acts as a metastasis suppressor gene in human ovarian carcinoma. Cancer Res 2002;62:6717–23.
7. Kyriakis JM, Avruch J. Mammalian mitogen-activated protein kinase signal transduction pathways activated by stress and inflammation. Physiol Rev 2001;81:807–69.
8. Pearson G, Robinson F, Beers Gibson T, et al. Mitogen-activated protein (MAP) kinase pathways: regulation and physiological functions. Endocr Rev 2001;22:153–83.
9. Yu D, Wolf JK, Scanlon M, et al. Enhanced c-erbB-2/neu expression in human ovarian cancer cells correlates with more severe malignancy that can be suppressed by E1A. Cancer Res 1993;53:891–8.
10. Hickson JA, Huo D, Vander Griend DJ, et al. The p38 kinases MKK4 and MKK6 suppress metastatic colonization in human ovarian carcinoma. Cancer Res 2006;66:2264–70.
11. Demicheli R, Pratesi G, Foroni R. The exponential-Gompertzian tumor growth model: data from six tumor cell lines *in vitro* and *in vivo*. Estimate of the transition point from exponential to Gompertzian growth and potential clinical implications. Tumori 1991;77:189–95.
12. Rygaard K, Spang-Thomsen M. Quantitation and gompertzian analysis of tumor growth. Breast Cancer Res Treat 1997;46:303–12.
13. Budzynski W, Radzikowski C. Cytotoxic cells in immunodeficient athymic mice. Immunopharmacol Immunotoxicol 1994;16:319–46.
14. Mule JJ, Jicha DL, Aebersold PM, et al. Disseminated human malignant melanoma in congenitally immune-deficient (bg/nu/xid) mice. J Natl Cancer Inst 1991;83:350–5.
15. De Feudis P, Vignati S, Rossi C, et al. Driving p53 response to Bax activation greatly enhances sensitivity to Taxol by inducing massive apoptosis. Neoplasia 2000;2:202–7.
16. Yaginuma Y, Westphal H. Abnormal structure and expression of the p53 gene in human ovarian carcinoma cell lines. Cancer Res 1992;52:4196–9.
17. Yaginuma Y, Hayashi H, Kawai K, et al. Analysis of the Rb gene and cyclin-dependent kinase 4 inhibitor genes (p16INK4 and p15INK4B) in human ovarian carcinoma cell lines. Exp Cell Res 1997;233:233–9.
18. Nakayama K, Nakayama N, Davidson B, et al. Homozygous deletion of MKK4 in ovarian serous carcinoma. Cancer Biol Ther 2006;5:630–4.
19. Lancaster JM, Dressman HK, Clarke JP, et al. Identification of genes associated with ovarian cancer metastasis using microarray expression analysis. Int J Gynecol Cancer 2006;16:1733–45.
20. Porras A, Zuluaga S, Black E, et al. P38 α mitogen-activated protein kinase sensitizes cells to apoptosis induced by different stimuli. Mol Biol Cell 2004;15:922–33.
21. Sarkar D, Su ZZ, Lebedeva IV, et al. mda-7 (IL-24) Mediates selective apoptosis in human melanoma cells by inducing the coordinated overexpression of the GADD family of genes by means of p38 MAPK. Proc Natl Acad Sci U S A 2002;99:10054–9.
22. el-Deiry WS, Tokino T, Velculescu VE, et al. WAF1, a potential mediator of p53 tumor suppression. Cell 1993;75:817–25.
23. Xiong Y, Hannon GJ, Zhang H, et al. p21 is a universal inhibitor of cyclin kinases. Nature 1993;366:701–4.
24. Dulic V, Beney GE, Frebourg G, et al. Uncoupling between phenotypic senescence and cell cycle arrest in aging p21-deficient fibroblasts. Mol Cell Biol 2000;20:6741–54.
25. Noda A, Ning Y, Venable SF, et al. Cloning of senescent cell-derived inhibitors of DNA synthesis using an expression screen. Exp Cell Res 1994;211:90–8.
26. Macleod KF, Sherry N, Hannon G, et al. p53-dependent and independent expression of p21 during cell growth, differentiation, and DNA damage. Genes Dev 1995;9:935–44.
27. Jost CA, Marin MC, Kaelin WG, Jr. p73 is a simian [correction of human] p53-related protein that can induce apoptosis. Nature 1997;389:191–4.
28. Chen CL, Ip SM, Cheng D, et al. P73 gene expression in ovarian cancer tissues and cell lines. Clin Cancer Res 2006;6:3910–5.
29. Dasari A, Bartholomew JN, Volonte D, et al. Oxidative stress induces premature senescence by stimulating caveolin-1 gene transcription through p38 mitogen-activated protein kinase/Sp1-mediated activation of two GC-rich promoter elements. Cancer Res 2006;66:10805–14.
30. Kim GY, Mercer SE, Ewton DZ, et al. The stress-activated protein kinases p38α and JNK1 stabilize

p21(Cip1) by phosphorylation. J Biol Chem 2002;277:29792–802.
31. Yee AS, Paulson EK, McDevitt MA, et al. The HBP1 transcriptional repressor and the p38 MAP kinase: unlikely partners in G_1 regulation and tumor suppression. Gene 2004;336:1–13.
32. Brugarolas J, Moberg K, Boyd S, et al. Inhibition of cyclin-dependent kinase 2 by p21 is necessary for retinoblastoma protein-mediated G_1 arrest after γ-irradiation. Proc Natl Acad Sci U S A 1999;96:1002–7.
33. Chin YE, Kitagawa M, Su WC, et al. Cell growth arrest and induction of cyclin-dependent kinase inhibitor p21 WAF1/CIP1 mediated by STAT1. Science 1996;272:719–22.
34. Choudhury AR, Ju Z, Djojosubroto MW, et al. Cdkn1a deletion improves stem cell function and lifespan of mice with dysfunctional telomeres without accelerating cancer formation. Nat Genet 2007;39:99–105.
35. Aguero MF, Facchinetti MM, Sheleg Z, et al. Phenoxodiol, a novel isoflavone, induces G_1 arrest by specific loss in cyclin-dependent kinase 2 activity by p53-independent induction of p21WAF1/CIP1. Cancer Res 2005;65:3364–73.
36. Lee B, Kim CH, Moon SK. Honokiol causes the p21WAF1-mediated G(1)-phase arrest of the cell cycle through inducing p38 mitogen activated protein kinase in vascular smooth muscle cells. FEBS Lett 2006;580:5177–84.
37. Iiizumi M, Bandyopadhyay S, Watabe K. Interaction of Duffy antigen receptor for chemokines and KAI1: a critical step in metastasis suppression. Cancer Res 2007;67:1411–4.
38. Bandyopadhyay S, Zhan R, Chaudhuri A, et al. Interaction of KAI1 on tumor cells with DARC on vascular endothelium leads to metastasis suppression. Nat Med 2006;12:933–8.
39. Rinker-Schaeffer CW, Hickson JA. Stopping cancer before it colonizes. Nat Med 2006;12:887–8.